ORIGINAL ARTICLE

10.2478/AMB-2026-0042

SYNTHESIS AND IN VITRO EVALUATION OF NEUROTOXICITY AND MAOA/B INHIBITORY EFFECTS OF NEW PYRROLYL-BASED FURAN, SUBSTITUTED FURAN AND INDOLE AZOMETHINE DERIVATES

M. Sharkov[1], M. Georgieva[1], M. Kondeva-Burdina[2]

[1]Department of Pharmaceutical Chemistry, Faculty of Pharmacy, Medical University – Sofia, Bulgaria
[2]Department of Pharmacology, Pharmacotherapy and Toxicology, Faculty of Pharmacy, Medical University – Sofia, Bulgaria

Abstract. *In this study the synthesis of three new N-pyrrolyl azomethine derivatives comprising furan, substituted furan and indole residues is presented. A classical Paal-Knorr cyclization was used for synthesis of the initial N-pyrrolyl hydrazine and the final azomethines were obtained in a micro synthesis scale, assuring about 69–76% yields, low harmful emissions and reagent economy. The compounds were elucidated by IR, 1H NMR and 13C NMR spectral analyses and the obtained results were consistent with the assigned structures. The purity of the substances was proven by TLC characteristics and corresponding melting points. In addition, the neurotoxicity and possible MAO-A and MAO-B inhibitory effects were elucidated in vitro. The obtained results indicated that the target molecules are with low neurotoxicity and no MAOA/B enzyme inhibiting effects.*

Key words: *pyrrole hydrazones, neurotoxicity, MAOA/B inhibition*

Corresponding author: *Magdalena Kondeva-Burdina, PhD, Department of Pharmacology, Pharmacotherapy and Toxicology, Faculty of Pharmacy, Medical University – Sofia, Bulgaria, email: mkondeva@pharmfac.mu-sofia.bg*

ORCID: *0000-0001-6776-0870*

Received: *10 September 2025;* ***Revised/Accepted:*** *08 January 2026*

INTRODUCTION

Neurodegenerative disorders (NDs), including Alzheimer's disease (AD), Parkinson's disease (PD), multiple sclerosis (MS), Huntington's disease (HD), and amyotrophic lateral sclerosis (ALS), are characterized by progressive neuronal and synaptic loss, often emerging later in life. The extent of neuronal degeneration closely correlates with clinical symptom onset and progression. In AD, for example, early hippocampal neuron loss impairs episodic memory. While several therapies are approved, most target symptoms rather than disease progression. Challenges such as the blood-brain barrier and adverse side effects limit therapeutic efficacy and contribute to poor survival outcomes [1].

MAO inhibitors (MAOIs), originally developed as antidepressants, have shown therapeutic potential in neurodegenerative disorders, including Alzheimer's disease (AD) and Parkinson's disease (PD) [2]. MAO exists in two isoforms, MAO-A and MAO-B, and is widely distributed on the outer mitochondrial membrane in mammalian cells. These isoforms metabolize neurotransmitters, such as dopamine, serotonin, and noradrenaline, and dysregulation of their activity has been associated

with various neuropsychiatric and neurodegenerative disorders, including AD and PD [3, 4, 5].

In AD, disturbances in monoaminergic systems – particularly serotonergic and dopaminergic – have been linked to altered MAO activity [5]. MAO catalyzes the oxidative deamination of biogenic amines, generating neurotoxic by-products, including hydrogen peroxide (H_2O_2), ammonia, and aldehydes, which may contribute to oxidative stress and disease progression. MAO-A is predominantly expressed in catecholaminergic neurons, while MAO-B is found in serotonergic neurons and glia. Autopsy studies reveal increased MAO-A and MAO-B activity in several brain regions during early and late AD stages [6]. Immunostaining shows elevated MAO-B in the hippocampus and cortex, while MAO-A is increased in the frontal pole and hypothalamus [7]. These alterations may result from transcriptional or post-transcriptional changes and are implicated in AD pathogenesis [5]. MAO activity correlates with cognitive dysfunction in AD. Monoamine neurotransmitter systems – particularly those involving norepinephrine (NE), serotonin (5-HT), and acetylcholine – are essential for attention, memory, orientation, and emotional regulation [8]. MAO-A preferentially degrades NE and 5-HT [9], while MAO-B targets substrates like phenylethylamine and benzylamine [10]. Dysregulation of MAO thus impairs neurotransmission, contributing to cognitive deficits through NE pathway disruption and cholinergic dysfunction [11].

Oxidative stress, partially driven by MAO-mediated ROS production, further exacerbates neurotransmitter dysfunction. Additionally, MAO activity is linked to neuroinflammation, which intensifies oxidative stress and promotes neurodegeneration [12]. Changes in monoamine metabolites such as homovanillic acid (HVA) and 5-hydroxyindoleacetic acid (5-HIAA) are associated with cognitive decline in AD models [13].

Elevated platelet MAO-B activity in AD patients correlates with disease severity, and its measurement may serve as a potential biomarker. MAO-B activity is also elevated in astrocytes surrounding amyloid plaques, suggesting a role in amyloid-β (Aβ) pathology [14]. MAO may contribute to APP cleavage via BACE and γ-secretase, promoting Aβ generation. Additionally, 5-HT receptor signaling (e.g., 5-HT2A, 5-HT2C, and 5-HT4) may modulate Aβ production [15].

Reactive astrocytic GABA synthesis via MAO-B impairs synaptic plasticity and memory function in AD models. Inhibition of MAO-B with drugs like selegiline has been shown to restore synaptic function and cognitive performance, despite the presence of Aβ pathology [16]. Although selegiline offers short-term cognitive benefits in AD, long-term efficacy remains limited [17].

Given the interplay between oxidative stress, neuroinflammation, and amyloid pathology, targeting MAO – especially MAO-B – presents a promising therapeutic strategy. MAOIs may reduce Aβ production and inflammation by modulating NF-κB signaling and cytokine expression. The design and development of selective MAOIs could offer new avenues for treating AD and related neurodegenerative disorders [18].

Nicotinamide adenine dinucleotide phosphate (NADPH), also known as reduced coenzyme II, plays a critical role in regulating redox homeostasis, mitigating neuroinflammation, and preserving mitochondrial function. Neurodegenerative disorders such as Alzheimer's disease (AD) and Parkinson's disease (PD) exhibit shared pathological hallmarks, including mitochondrial dysfunction, oxidative stress, and chronic neuroinflammation, often triggered by the accumulation of misfolded protein aggregates [19].

NADPH and Monoamine Oxidase (MAO) play distinct but interconnected roles in cellular processes. NADPH is a coenzyme that serves as a key reducing agent in anabolic reactions and supports antioxidant defense by maintaining redox balance [20]. In contrast, MAO is an enzyme responsible for the oxidative deamination of monoamines, generating aldehydes, ammonia, and hydrogen peroxide [21]. While NADPH does not directly participate in MAO's enzymatic activity, it may indirectly affect MAO function through its involvement in redox signaling and the cellular response to oxidative stress [22]. Thus, finding new approaches combining activities against these neurodegeneration-sensitive targets is of great importance for establishing successful therapy of neurodegenerative conditions.

The purpose of this investigation is to evaluate the possible neurotoxicity and MAOA/B inhibitory effects of newly synthesized N-pyrrolyl hydrazide-hydrazones.

MATERIALS AND METHODS

General

The melting points were determined on Kruss M5000 and are not corrected. The synthesis progress was controlled by TLC on aluminum sheets Silica gel 60 F254 (Merck, Darmstadt, Germany), using $CHCl_3$/CH_3CH_2OH as a mobile phase. Yields were calculated for purified products. The IR spectra were recorded on a Nicolet iS10 FT-IR spectrometer with a Smart iTR adapter (Thermo Fisher Scientific, USA). The 1H NMR spectra were registered at 250 MHz on spectrometer Bruker-Spectrospin WM250MHz

(Faenlanden, Switzerland) as δ (ppm) relative to TMS as internal standard with DMSO-d6 as a solvent (20°C); coupling constants (J) are expressed in Hertz (Hz). All OH and NH protons were D2O exchangeable. Available solvents and reactants were acquired from commercial suppliers (Sigma-Aldrich; Fluka) and applied without purification.

General procedure for the synthesis of the targeted hydrazones:

To 1.5 mmol of the initial carbohydrazide **13** were dissolved 1.5 mmol of any of the carbonyl partners **h, i** or **j** in glacial acetic acid in a round bottom flask of 20 ml. The mixture was stirred at 100 oC for 40-50 min to complete the reaction under TLC-control. The products were isolated after pouring into cold water and recrystallized from ethanol where necessary.

The IUPAC names* of the newly synthesized hydrazones, together with the interpretation of their IR and 1H NMR spectra, are presented below:

*(E)-ethyl 5-(4-bromophenyl)-1-(4-(2-(furan-2-ylmethylene)hydrazinyl)-4-oxobutyl)-2-methyl-1H-pyrrole-3-carboxylate **(15h)**:* IR [cm^{-1}]: 3120 (OH and NH), 1695 ($COOC_2H_5$), 1640 (Amide I), 1520 (Amide II), 1240 (C-O), 810 (p-disubstituted C_6H_4); ^{1}H NMR (at 400 MHz, in $DMSOd_6$): 1.28 [s, 3H, CH_2CH_3], 2.03 [t, 2H, $CH_2CH_2CH_2$], 2.45 [s, 3H, CH_3(2)], 2.38 [s, 2H, $CH_2CH_2CH_2$], 4.26 [s, 2H, $N(CH_2)$], 4.32 [s, 2H, CH_2CH_3], 6.4 [s, 1H, H(4)], 7.05 [s, 1H, NH-N], 7.12 [s, 1H, H(3″)], 7.61 [s, 1H, H(4″)], 7.73 [s, 2H, H(3'), H(5')], 7.8 [s, 2H, H(2'), H(6')], 8.27 [s, 1H, CH=N]; ^{13}C NMR (100 MHz, $DMSOd_6$): δ 170.4, 163.0, 144.4, 132.06 (2C), 125.3 (2C), 134.6, 118.9, 116.3, 114.4, 112.6, 110.3, 51.5, 43.6, 39.4, 26.3, 14.9 and 11.4.

*(E)-ethyl 5-(4-bromophenyl)-2-methyl-1-(4-(2-((5-nitrofuran-2-yl)methylene)hydrazinyl)-4-oxobutyl)-1H-pyrrole-3-carboxylate **(15i):*** IR [cm-^{1}]: 2979 (CH_3 and CH_2), 1682 ($COOC_2H_5$), 1602 (Amide I), 1521 (Amide II), 1242 (C-O), 809 (p-substituted C_6H_4), 544 (C-Br); ^{1}H NMR (at 400 MHz, in $DMSOd_6$): 1.26 [s, 3H, CH_2CH_3], 2.06 [t, 2H, $CH_2CH_2CH_2$], 2.47 [s, 3H, CH_3(2)], 2.35 [s, 2H, $CH_2CH_2CH_2$], 4.16 [s, 2H, $N(CH_2)$], 4.3 [s, 2H, CH_2CH_3], 6.4 [s, 1H, H(4)], 7.0 [s, 1H, NH-N], 7.09 [s, 1H, H(3″)], 7.59 [s, 1H, H(4″)], 7.68 [s, 2H, H(3'), H(5')], 7.71 [s, 2H, H(2'), H(6')], 8.25 [s, 1H, CH=N]; ^{13}C NMR (100 MHz, $DMSOd_6$): δ 173.4, 164.0, 163.3, 132.06 (2C), 125.3 (2C), 134.6, 116.7, 114.3, 114.4, 114.7, 112.3, 51.5, 43.6, 39.4, 26.3, 14.9 and 11.4.

(E)-ethyl 5-(4-bromophenyl)-2-methyl-1-(4-oxo-4-(2-((3-oxoindolin-2-yl)methylene)hydrazinyl) butyl)-1H-pyrrole-3-carboxylate **(15j):** IR [cm^{-1}]: 3119 (OH and NH), 1689 ($COOC_2H_5$), 1640 (Amide I), 1520 (Amide II), 1240 (C-O), 810 (p-disubstituted C_6H_4); ^{1}H NMR (at 400 MHz, in $DMSOd_6$): 1.27 [s, 3H, CH2CH3], 2.03 [t, 2H, $CH_2CH_2CH_2$], 2.45 [s, 3H, CH_3(2)], 2.38 [s, 2H, $CH_2CH_2CH_2$], 4.0 [s, 1H, NH], 4.26 [s, 2H, $N(CH_2)$], 4.32 [s, 2H, CH_2CH_3], 6.4 [s, 1H, H(4)], 7.05 [s, 1H, NH-N], 7.14 [s, 2H, H(3'), H(5')], 7.20 [s, 1H, H(7″)], 7.34 [s, 1H, H(3″)], 7.78 [s, 12H, H(4″), H(6″)], 7.8 [s, 2H, H(2'), H(6')], 8.27 [s, 1H, CH=N]; ^{13}C NMR (100 MHz, $DMSOd_6$): δ 187.4, 167.0, 163.0, 144.4, 142.7, 135.5, 132.06 (2C), 126.3, 125.3 (2C), 134.6, 118.9, 116.3, 114.4, 112.6, 110.3, 51.5, 43.6, 39.4, 26.3, 14.9 and 11.4.

Pharmacological studies

The necessary for the pharmacological evaluations reagents and buffers including Percoll reagent, Buffer B, glucose, 3-(4,5-dimethylthiazol-2-yl)-2,5-diphenyltetrazolium bromide (MTT), dimethyl sulfoxide (DMSO), 5,5′-dithiobis-(2-nitrobenzoic acid) (DTNB), trichloroacetic acid, 0.1 M Tris buffer containing: 0.1 mM dithiothreitol, 0.1 mm phenylmethylsulfonyl fluoride, 0.2 mM ethylendiamine tetra acetic acid (EDTA), 1.15% potassium chloride (KCl) and 20% (v/v) glycerol (pH 7.4) and the corresponding Assay kits for evaluation of MAO inhibitory activity were purchased from Sigma Aldrich.

Animals

A total of 10 animals were used in the experiments. The animals were obtained from the National Breeding Centre of the Bulgarian Academy of Sciences, Sofia, Bulgaria and kept under standard conditions in plexiglass cages with free access to water and food and 12 h/12 h light/dark regime at 20-25°C. Twelve hours before each specific study, the animals' food was withdrawn. The experiments were conducted in accordance with the Ordinance No. 15 on Minimum Requirements for the Protection and Welfare of Experimental Animals (SG No. 17, 2006), the European Regulation for the Handling of Experimental Animals and the Permission №304/valid until 28.06.2026 from the Bulgarian Food Safety Agency.

Preparation of rat brain synaptosomes and mitochondria

Synaptosomes and mitochondria were obtained by multiple, subcellular fractionation using a Percoll gradient [23]. The necessary brain homogenate was prepared and centrifuged at 1,000 x g for 5 min at +4 °C. After centrifugation, the supernatants were collected and centrifuged again at 1,000 rpm for 5 min at +4°C. The supernatants from the two centrifugations were mixed and distributed into 4 tubes. The tubes were centrifuged at 10,000 x g for 20 min

[1] *ACD/Name Version 2.51*

at +4 °C three times. The last two centrifugations were for purification of synaptosomes and mitochondria.

Isolation of the corresponding synaptosomal and mitochondrial fractions

The isolation of the required fractions was based on formation of a colloidal solution of silicon (Percoll), as per the procedure including: 1. Preparation of a 90% stock solution of Percoll, followed by preparation of two Percoll solutions of different percentages: 16% and 10%. 4 mL of each of the prepared 16% and 10% Percoll solution was placed in six test tubes. A 90% Percoll (7.5 % Percoll) was added to the precipitate obtained from the previous step from the last centrifugation. The obtained mixtures in all 12 tubes were centrifuged for 20 min at 15,000 x g +4°C. After centrifugation, three layers are formed in the tubes. The bottom layer contains mitochondria, the top layer contains lipids, and the middle layer – at the 16% to 10% Percoll limit – contains synaptosomes. The respective layer from each tube is removed through a glass pasteurizer and collected into one. Buffer B + glucose is added to it. The mixture was centrifuged at 10,000 x g for 20 min at +4°C. Thus, the isolation buffer is exchanged with the incubation buffer. After centrifugation, the pellet where the synaptosomes are is mixed and made up with buffer B + glucose.

Incubation of synaptosomes

Synaptosomes and mitochondria were incubated with the test substances, at a concentration of 50 μM, for 1 h.

MTT assay to assess synaptosomal viability

After 1 h incubation with the substances, synaptosomes were centrifuged on a microcentrifuge for 1 min at 15,000 x g. The pellet was mixed gently with buffer B + glucose, and the supernatant was discarded to prevent oxidation of MTT. Centrifuge again at 15,000 x g for 1 min. After the second wash, buffer B + glucose were added to the pellet. To the 'washed' synaptosomes, 60 μL of MTT solution were added. The plates were incubated with the MTT solution at 37 ºC for 10 min. After incubation, the samples were centrifuged at 15,000 x g for 2 min. The excess liquid was removed and a DMSO solution was used to dissolve the formed formazan crystals. After dissolution, the amount of formazan is measured spectrophotometrically at λ = 580 nm [24].

Determination of reduced glutathione (GSH) in isolated brain synaptosomes

After precipitation of the proteins with trichloroacetic acid, the thiol groups in the supernatant were determined by DTNB, which produced a yellow-colored compound that absorbs light at λ = 412 nm. After incubation, synaptosomes were centrifuged at 400 x g for 3 min. The supernatant was removed and the pellet taken for GSH determination. It was treated with 5% trichloroacetic acid, then left for 10 min on ice. Centrifuge at 8000 x g for 10 min (2°C). The supernatant is taken for GSH determination and frozen at -20°C. Immediately before measurement, the samples are neutralised with 5N NaOH [25].

Determination of malondialdehyde (MDA) production in brain mitochondria [26]

To the mitochondria was added 0.3 ml of 0.2% thiobarbituric acid and 0.25 ml of sulfuric acid (0.05 M), and the mixture was boiled for 30 minutes. After boiling, the tubes were placed on ice and 0.4 ml of n-butanol was added to each, then centrifuged at 3,500 x g for 10 minutes. The amount of MDA was determined spectrophotometrically at 532 nm.

Determination of GSH level in brain mitochondria [26]

After incubating the mitochondria with the substances, the reaction was stopped with 5% trichloroacetic acid, and each sample was homogenized with the acid and left on ice. After centrifugation of the homogenate at 6,000 x g, a 0.04 % solution of DTNB was added to the supernatant to give a yellow color, the determination being spectrophotometric at 412 nm.

Isolation of brain microsomes [27]

The brain was homogenized in 9-volume parts of 0.1 M Tris buffer containing: 0.1 mM Dithiothreitol, 0.1 mM Phenylmethylsulfonyl fluoride, 0.2 mM EDTA, 1.15% KCl and 20% (v/v) glycerol (pH 7.4). The resulting homogenate was centrifuged twice at 17,000 x g for 30 min. The supernatants from the two centrifugations were pooled and centrifuged twice at 100,000 x g for 1 h. The pellet was frozen in 0.1 M Tris buffer.

Determination of MDA in brain microsomes [28]

After completion of incubation of the microsomes with the substances, the reaction was stopped by the addition of 0.5 ml of 20% trichloroacetic acid, followed by 0.5 ml of 0.67% thiobarbituric acid. The ongoing reactions are associated with the formation of a colored complex between the malondialdehyde formed and thiobarbituric acid. The determination of MDA was spectrophotometric at 535 nm. A molar extinction coefficient of 1.56 x 105 M^{-1} cm^{-1} was used for the calculation.

Determination of human recombinant MAOA/B enzyme activity

The activity of recombinant human MAOA/B was determined fluorimetrically. Tyramine hydrochloride was used as substrate. The activity is determined by detection of H_2O_2 production. This production

is, in turn, reported by binding to horseradish peroxidase using N-acetyl-3,7-dihydroxyphenoxazine (AmplexRed) [29]. Working solutions of the test substances, reagents and human recombinant MAOA/B enzyme (hMAOA/B) were prepared in reaction buffer according to the manufacturer's instructions. A pure working solution of MAOA/B in reaction buffer, a working solution of MAOA/B containing hydrogen peroxide, and a pure reaction buffer were used as controls. Substances were applied at a final concentration of 1 μM. The substances, together with hMAOB, were placed in a 96-well plate (8 samples for each substance), and then the plate was placed in an incubator for 30 min (in the dark, at 37°C). Fluorimetric readings were performed in a Synergy 2 Microplate Reader, at two wavelengths (570 nm and 690 nm).

Statistical methods

The results of the experiments performed on isolated brain synaptosomes, mitochondria and microsomes were statistically processed using the 'MEDCALC' program using the non-parametric Mann-Whitney method at significance levels $P < 0.05$; $P < 0.01$ and $P < 0.001$.

The results obtained from hMAOA/B activity were statistically processed using GraphPad Prism 5.0 software.

RESULTS

Chemistry

The initial for the synthesis N-pyrrolyl hydrazine was synthesized according to a procedure explained elsewhere [30] via classical Paal-Knorr cyclization, followed by esterification of the initial carboxylic acids and its hydrazinolysis as presented on Figure 1.

The Schiff bases (comprising an azomethine group (-CH=N-)) were synthesized by a nucleophilic addition reaction of the corresponding aldehydes (h and i) and the ketone j and the initial N-pyrrolyl hydrazine as by the procedure defined on Figure 2 with any of the carbonyl compounds presented on Figure 3:

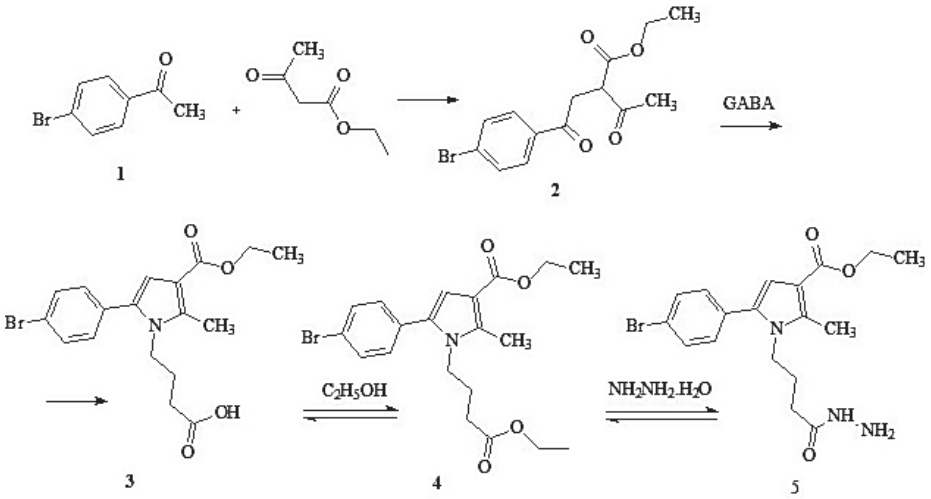

Fig. 1. Synthesis of the used N-pyrrolyl hydrazine 5

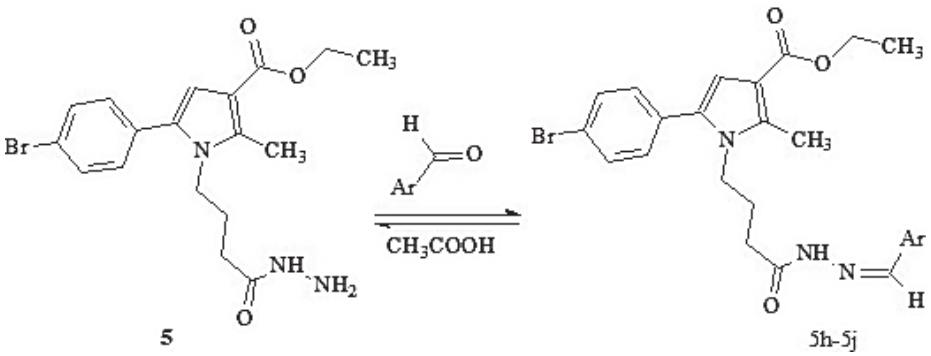

Fig. 2. General synthesis of the target compounds

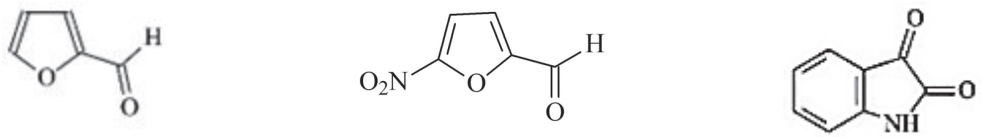

h **i** **j**

Fig. 3. Used carbonyl compounds

The purity of the new compounds was confirmed by TLC analysis and their structure was elucidated, with IR, 1H NMR and 13C NMR spectral data. The corresponding melting points, TLC characteristics and yields are presented in Table 1.

Table 1. Melting points, TLC characteristics (Rf/(CHCl3:C2H5OH) and yields (%)

Compound ID	Melting points	TLC characteristics (Rf/(CHCl3:C2H5OH)	Yields (%)
15h	134.8–135.9	0.60	72
15i	131.7–132.9	0.58	69
15j	95.4–96.3	0.76	76

In silico assessment of physicochemical properties and possible biological effects of the new azomethine derivates. Prediction of pharmacokinetic properties

Web-based online servers for prediction of pharmacokinetics of the target hydrazones were applied as a tool for preliminary evaluation of the applicability of the designed azomethines. The results from the performed calculations using two web-based tools – Milinspiration Chemisnformatics [31] and Molsoft L.L.C. Molecular properties predictor [32] – are presented in Table 2.

Table 2. Some calculated pharmacokinetic parameters

ID	Molinspiration Cheminformatics									Molecular Properties and Drug-likeness				
	miLogP	TPSA	natoms	MW	nON	nOHNH	nviolations	nrotb	volume	MolLogS	pKa of most Basic/Acidic group	BB Score*	Number of stereo centers:	Drug-likeness model score:
15h	4.63	85.84	31	486.37	7	1	0	10	394.62	-4.56	0.73/12.24	3.42	0	0.39
15i	4.71	131.66	34	531.36	10	1	1	11	417.96	-4.23	0.78/12.18	1.88	0	0.06
15j	4.05	101.8	36	551.44	8	2	1	10	450.43	-4.23	1.83/7.97	2.58	1	0.89

**The Blood-Brain Barrier (BBB) Score: 6-High,0-Low [33].*

Table 3. Prediction of interaction of the test compounds with the defined targets.

Alzheimer target	IDs	Predicted Outcome	Probability	Probability Active	Probability Inactive	Predicted Reliability
Alzheimer – COX2	15h	Inactive	0.8	0.2	0.8	reliable
	15i	Inactive	0.5	0.2	0.8	unreliable
	15j	Inactive	1.0	0.0	1.0	unreliable
Alzheimer – iNOS	15h	Inactive	0.8	0.2	0.8	unreliable
	15i	Inactive	1.0	0.0	1.0	unreliable
	15j	Inactive	0.6	0.4	0.6	unreliable
Alzheimer – NADPH	15h	Active	1.0	1.0	0.0	unreliable
	15i	Active	1.0	1.0	0.0	unreliable
	15j	Active	1.0	1.0	0.0	unreliable
Alzheimer – JNK-3	15h	Inactive	1.0	0.0	1.0	unreliable
	15i	Inactive	1.0	0.0	1.0	unreliable
	15j	Inactive	0.6	0.4	0.6	unreliable
Alzheimer – PDE5	15h	Inactive	1.0	0.0	1.0	unreliable
	15i	Inactive	1.0	0.0	1.0	unreliable
	15j	Inactive	1.0	0.0	1.0	unreliable

Prediction of biological activity

In addition, we made an attempt to identify the appearance of possible effect of the target compounds against some neurodegenerative disorders, like Alzheimer's disease. As a predictive tool we applied the online platform MolPredictX [34]. The results of the predictions are presented in Table 3.

Pharmacological evaluations
Neurotoxicity assessment
Effect on isolated rat brain synaptosomes

When administered alone, at a concentration of 50 μM, to brain synaptosomes, the test substances **(15h-15j)** showed a statistically significant weak neurotoxic effect compared to the control (untreated synaptosomes). They slightly decreased synaptosomal viability and reduced glutathione level (Figure 4A and 4B).

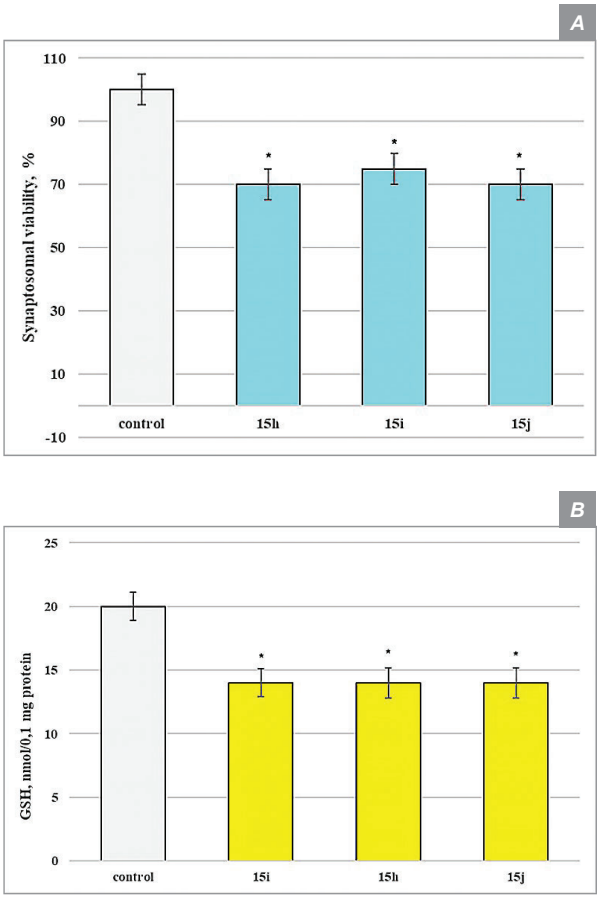

* P < 0,05 against the control (non-treated synaptosomes) * P < 0,05 against the control (non-treated synaptosomes)

Fig. 4. Effect of the tested hydrazones on synaptosomal vitality (A) and GSH levels (B)

All evaluated compounds revealed a comparable towards isolated synaptosomes weak neurotoxic effect.

Effect on isolated rat brain microsomes

Self-administered, at a concentration of 50 μM, to brain microsomes, the test substances **(15h-15j)** again exhibited a statistically significant weak neurotoxic effect, relative to the control (untreated microsomes).

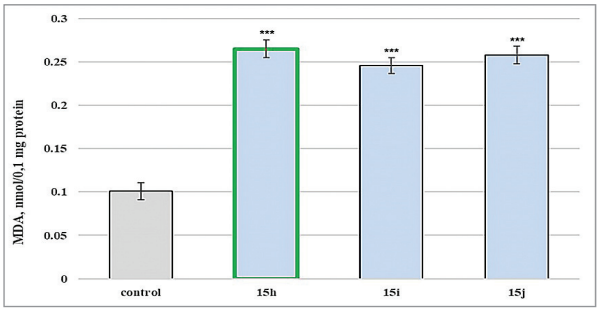

*** P < 0.001 vs control (untreated microsomes)

Fig. 5. Effect of the tested hydrazones on microsomal MDA levels

The increase in the production of malondialdehyde (MDA), used as a marker of lipid peroxidation (Figure 5) identified compound **15i** with the weakest neurotoxic effect in isolated microsomes.

Effect on isolated rat brain mitochondria

The performed experiments showed that when applied alone, at a concentration of 50 μM, to brain mitochondria, the test substances **(15h-15j)** exhibited a statistically significant weak neurotoxic effect, relative to the control (untreated mitochondria).

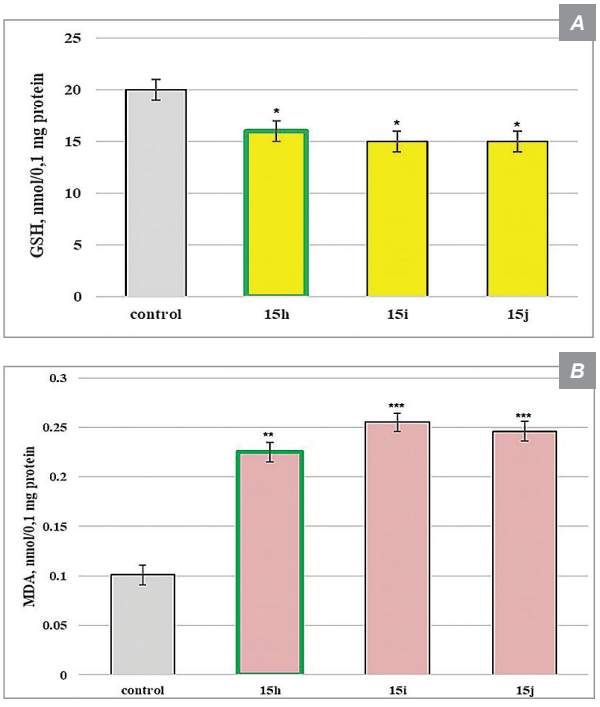

* P < 0,05 against the control (untreated mitochondria)
*** P < 0.001 vs control (untreated mitochondria)

Fig. 6. Effect of the tested hydrazones on mitochondria GSH (A) and MDA levels (B)

They slightly decreased reduced glutathione (GSH) level and increased malondialdehyde (MDA) production (Figure 6A and 6B). The substance with the weakest neurotoxic effect was **15h**.

In vitro MAOA/B inhibitory activity

As a result of the performed pharmacological and toxicological studies of the newly synthesized hydrazones, it was found that the evaluated molecules show minimal neurotoxicity on subcellular fractions (isolated rat brain synaptosomes, mitochondria and microsomes).

These results pointed our attention towards assessment for their possible inhibitory effects on the MAO isoforms type A and B.

The inhibitory effect on both MAOA and MAOB isoforms was evaluated in vitro and the corresponding results are presented on Figure 7A and 7B, respectively.

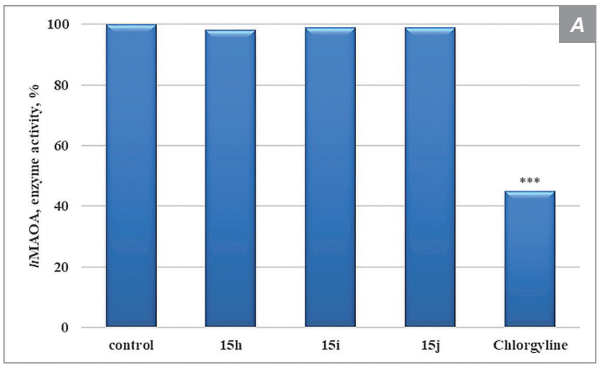

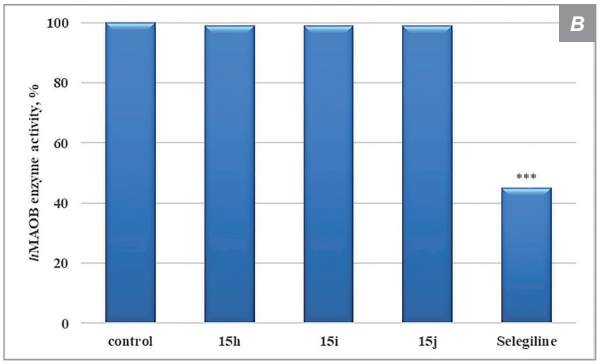

*** P < 0.001 vs control (pure hMAOA)
*** P < 0.001 vs control (pure hMAOB)

Fig. 7. Effect of newly synthetized hydrazones (at concentration 1 μM), on the activity of human recombinant MAOA enzyme (hMAOA) (A) and human recombinant MAOB enzyme (hMAOB) (B), respectively

All of the newly synthesized hydrazones (at concentration 1 μM), DID NOT reveal statistically significant inhibitory effect on human recombinant MAOA and/or MAOB enzymes (hMAOA/B), compared to the controls (pure hMAOA and hMAOB, respectively) (Figure 7). Only clorgyline, which is a classical MAOA inhibitor, revealed statistically significant inhibitory effect by decreasing the enzyme activity with 45%, compared to the control (pure hMAOA enzyme) (Figure 7A). In means of hMAOB, only the selective MAOB inhibitor selegiline was found to express 45% inhibition (Figure 7B).

DISCUSSION

Chemistry

The target products were synthesized in micro synthesis conditions, ensuring about 69-76% yields, low harmful emissions and reagent economy. The results from the structural elucidations indicated high consistency with the theoretically assigned values.

In silico assessment of physicochemical properties and possible biological effects of the new azomethine derivates.

The calculated results (Table 2) show that two of the designed compounds do not comply with Lipinski's rule of 5 regarding the corresponding molecular weight. In one of the representatives (15j) is possible appearance of stereoisomerism due to presence of a stereo center.

According to the presented data 15h is with highest BBB permeability, while 15j is characterized by the best drug-like properties.

The presented calculations (Table 3) indicate that the tested azomethines are expected to be active against Alzheimer's NADPH enzyme system. This should be considered in the future development of agents designed as therapy for Alzheimer's disease due to the recently evaluated influence between the activity of NADPH and MAO. It is found that NADPH and MAO participate in distinct yet interconnected cellular functions. NADPH is essential for maintaining redox balance and supporting antioxidant defenses, whereas MAO plays a key role in monoamine metabolism and contributes to oxidative stress through the production of reactive oxygen species (ROS). Their interplay is complex: NADPH can modulate MAO activity indirectly via redox signaling, while MAO-derived ROS can, in turn, influence the cellular redox environment [19].

Pharmacological evaluations

Neurotoxicity assessment

In attempt to indicate the mechanism of neurological affect, the target compounds were tested on isolated rat-brain synaptosomes, microsomes and mitochondria. The neurotoxicity was determined by evaluation of the synaptosomal viability and the effect of the test molecules on the corresponding biomarkers affecting the functional-metabolic status of the sub-cellular

fractions, expressed as decrease in the glutathione (GSH) levels and increase in the malondialdehyde (MDA) production.

The mitochondrial dysfunction hypothesis suggests that dysregulation in mitochondrial function may lead to neurodegeneration, as mitochondria have a dual role in regulation – as a source of ROS and an antioxidant. Since mitochondria are the site of electron transport processes, they are a major source of ROS that can lead to further mitochondrial damage and more pronounced neurodegeneration [35]. This aimed our research into evaluation of the mitochondria effect of the tested hydrazones.

In vitro MAOA/B inhibitory activity

Although MAO-B inhibitors are primarily used in the treatment of PD, dual MAOA/B inhibition is a relatively understudied treatment strategy that may have potential benefits. By inhibiting both isozymes, it is possible to reduce the level of several toxic metabolites, and to protect different types of neurons, as well as to modulate different neurotransmitter systems. However, the search for new and more effective antiparkinsonian agents continues.

The results indicated lack of activity against both isoforms, which defines lack of selectivity towards the enzymes and determines that the introduction of a furanyl, substituted furanyl and/or indolyl residue in the carboxylic fragment lead to lack of possible MAO inhibitory effects. This points the further developments towards excluding this type of residues in the design of such agents.

CONCLUSION

The performed pharmacological and toxicological studies on subcellular fractions (isolated rat brain synaptosomes, mitochondria and microsomes) of derivatives **15h – 15j**, defined that when administered alone, at a concentration of 50 μM, all substances exhibited a weak neurotoxic effect relative to the control (untreated subcellular fractions). The evaluated substances, at a concentration of 1 μM, did not exhibit inhibitory activity neither on MAOA, nor on MAOB enzyme. The reason for lack of MAO effect may be due to the introduction of a furanyl, substituted furanyl and/or indolyl residue in the carboxylic fragment in the azomethine molecule. This points the further developments towards excluding this type of residues in the design of such agents.

Acknowledgement: *This work was supported by the Medical Science Council of Medical University – Sofia, Grant No.:D-113/29.05.2024.*

Ethical statement: *The experiments were conducted in accordance with the Ordinance No. 15 on Minimum Requirements for the Protection and Welfare of Experimental Animals (SG No. 17, 2006), the European Regulation for the Handling of Experimental Animals and the Permission №304/valid until 28.06.2026 from the Bulgarian Food Safety Agency.*

Conflict of interest: *The authors declare that there is no conflict of interest regarding this article.*

REFERENCES

1. Dnyandev GG, Sugandhi VV, Jha SK, et al. Neurodegenerative disorders: Mechanisms of degeneration and therapeutic approaches with their clinical relevance. Ageing Res Rev, 2024, 99:102357. doi: 10.1016/j.arr.2024.102357.
2. Youdim MBH, Edmondson D, Tipton KF. The therapeutic potential of monoamine oxidase inhibitors. Nat Rev Neurosci, 2006, 7(4):295-309. doi: 10.1038/nrn1883.
3. Hong R, Li X. Discovery of monoamine oxidase inhibitors by medicinal chemistry approaches. Medchemcomm, 2018, 10(1):10-25. doi: 10.1039/c8md00446c.
4. Park JH, Ju YH, Choi JW, et al. Newly developed reversible MAO-B inhibitor circumvents the shortcomings of irreversible inhibitors in Alzheimer's disease. Sci Adv, 2019, 5(3):eaav0316. doi: 10.1126/sciadv.aav0316.
5. Manzoor S, Hoda N. A comprehensive review of monoamine oxidase inhibitors as anti-Alzheimer's disease agents: A review. Eur J Med Chem, 2020, 206:112787. doi: 10.1016/j.ejmech.2020.112787.
6. Cai Z. Monoamine oxidase inhibitors: promising therapeutic agents for Alzheimer's disease (Review). Mol Med Rep, 2014, 9(5):1533-1541. doi: 10.3892/mmr.2014.2040.
7. Burke WJ, Li SW, Schmitt CA, et al. Accumulation of 3,4-dihydroxyphenylglycolaldehyde, the neurotoxic monoamine oxidase A metabolite of norepinephrine, in locus ceruleus cell bodies in Alzheimer's disease: mechanism of neuron death. Brain Res, 1999, 816(2):633-637. doi: 10.1016/s0006-8993(98)01211-6.
8. Knittel J, Itani N, Schreckenberg R, et al. Monoamine Oxidase A contributes to serotonin- but not norepinephrine-dependent damage of rat ventricular myocytes. Biomolecules, 2023, 13(6):1013. doi: 10.3390/biom13061013.
9. Sung JS, Kim S, Jung J, et al. Monoamine Oxidase-A (MAO-A) inhibitors screened from the autodisplayed Fv-antibody library. ACS Pharmacol Transl Sci, 2023, 7(1):150-160. doi: 10.1021/acsptsci.3c00204.
10. Baweja GS, Gupta S, Kumar B, et al. Recent updates on structural insights of MAO-B inhibitors: a review on target-based approach. Mol Divers, 2024, 28(3):1823-1845. doi: 10.1007/s11030-023-10634-6.
11. Davis SE, Cirincione AB, Jimenez-Torres AC, Zhu J. The Impact of neurotransmitters on the neurobiology of neurodegenerative diseases. Int J Mol Sci, 2023, 24(20):15340. doi: 10.3390/ijms242015340.
12. Dash UC, Bhol NK, Swain SK, et al. Oxidative stress and inflammation in the pathogenesis of neurological disorders: Mechanisms and implications. Acta Pharm Sin B, 2025, 15(1):15-34. doi: 10.1016/j.apsb.2024.10.004.
13. Gallo A, Pillet LE, Verpillot R. New frontiers in Alzheimer's disease diagnostic: Monoamines and their derivatives in biological fluids. Exp Gerontol, 2021, 152:111452. doi: 10.1016/j.exger.2021.111452.

14. Schedin-Weiss S, Inoue M, Hromadkova L, et al. Monoamine oxidase B is elevated in Alzheimer disease neurons, is associated with γ-secretase and regulates neuronal amyloid β-peptide levels. Alzheimers Res Ther, 2017, 9(1):57. doi: 10.1186/s13195-017-0279-1.
15. Jaisa-Aad M, Muñoz-Castro C, Healey MA, et al. Characterization of monoamine oxidase-B (MAO-B) as a biomarker of reactive astrogliosis in Alzheimer's disease and related dementias. Acta Neuropathol, 2024, 147(1):66. doi: 10.1007/s00401-024-02712-2.
16. Naffaa MM. Monoamine Oxidase B in astrocytic GABA synthesis: a central mechanism in neurodegeneration and neuroinflammation. J Cell Signal, 2025, 6(2):53-70.
17. Marucci G, Buccioni M, Dal Ben D, et al. Efficacy of acetylcholinesterase inhibitors in Alzheimer's disease. Neuropharmacology, 2021, 190:108352. doi: 10.1016/j.neuropharm.2020.108352.
18. Rahman MS, Uddin MS, Rahman MA, et al. Exploring the role of monoamine oxidase activity in aging and Alzheimer's Disease. Curr Pharm Des, 2021; 27(38):4017-4029. doi: 10.2174/1381612827666210612051713.
19. Yang DC, Cheng Y, Lin F. NADPH and Alzheimer's Disease and Parkinson's Disease. In: Qin ZH (eds) Biology of Nicotinamide Coenzymes. 2025, Springer, Singapore. https://doi.org/10.1007/978-981-97-9877-3_39.
20. Giménez-Xavier P, Gómez-Santos C, Castaño E, et al. The decrease of NAD(P)H has a prominent role in dopamine toxicity. Biochim Biophys Acta, 2006, 1762(5): 564-574. doi: 10.1016/j.bbadis.2006.02.003.
21. Kaludercic N, Arusei RJ, Di Lisa F. Recent advances on the role of monoamine oxidases in cardiac pathophysiology. Basic Res Cardiol, 2023, 118(1):41. doi: 10.1007/s00395-023-01012-2.
22. Iacovino LG, Reis J, Mai A, et al. Diphenylene iodonium is a noncovalent MAO inhibitor: a biochemical and structural analysis. Chem Med Chem, 2020, 15(15):1394-1397. doi: 10.1002/cmdc.202000264.
23. Taupin P, Zini S, Cesselin F, et al. Subcellular fractionation on Percoll gradient of mossy fiber synaptosomes: morphological and biochemical characterization in control and degranulated rat hippocampus. J Neurochem, 1994, 62(4):1586-1595. doi: 10.1046/j.1471-4159.1994.62041586.x.
24. Mungarro-Menchaca X, Ferrera P, Morán J, Arias C. β-Amyloid peptide induces ultrastructural changes in synaptosomes and potentiates mitochondrial dysfunction in the presence of ryanodine. J Neurosci Res, 2002, 68(1):89-96. doi: 10.1002/jnr.10193.
25. Robyt JF, Ackerman RJ, Chittenden CG. Reaction of protein disulfide groups with Ellman's reagent: A case study of the number of sulfhydryl and disulfide groups in Aspergillus oryzae α-amylase, papain, and lysozyme. Arch Biochem Biophys, 1971, 147(1):262-269. doi: 10.1016/0003-9861(71)90334-1.
26. Shirani M, Alizadeh S, Mahdavinia M, Dehghani MA. The ameliorative effect of quercetin on bisphenol A-induced toxicity in mitochondria isolated from rats. Environ Sci Poll Res, 2019, 26(8):7688-7696. doi: 10.1007/s11356-018-04119-5.
27. Ravindranath V, Anandatheerthavarada HK. Preparation of brain microsomes with cytochrome P450 activity using calcium aggregation method. Anal Biochem, 1990, 187(2):310-313. doi: 10.1016/0003-2697(90)90461-h.
28. Mansuy D, Sassi A, Dansette PM, Plat M. A new potent inhibitor of lipid peroxidation in vitro and in vivo, the hepatoprotective drug anisyldithiolthione. Biochem Biophys Res Commun, 1986, 135(3):1015-1021. doi: 10.1016/0006-291x(86)91029-6.
29. Bautista-Aguilera OM, Esteban G, Bolea I, et al. Design, synthesis, pharmacological evaluation, QSAR analysis, molecular modeling and ADMET of novel donepezil-indolyl hybrids as multipotent cholinesterase/monoamine oxidase inhibitors for the potential treatment of Alzheimer's disease. Eur J Med Chem, 2014, 21(75):82-95. doi: 10.1016/j.ejmech.2013.12.028).
30. Georgieva M, Sharkov M, Mateev E, et al. Classical Paal-Knorr cyclization for synthesis of pyrrole-based aryl hydrazones and in vitro/in vivo evaluation on pharmacological models of Parkinson's disease. Molecules, 2025, 30: 3154. doi:10.3390/molecules30153154.
31. Molinspiration cheminformatics. [Internet], Accessed on September 2025. Available from: https://www.molinspiration.com/cgi/properties)
32. Abagyan R, Totrov M. High-throughput docking for lead generation. Curr Opinion Chem Biol, 200, 5(4):375-382 (https://molsoft.com/mprop/)
33. Gupta M, Lee HJ, Barden CJ, Weaver DF. The Blood-Brain Barrier (BBB) score. J Med Chem, 2019, 62(21):9824-9836. doi: 10.1021/acs.jmedchem.9b01220.
34. Scotti MT, Herrera-Acevedo C, de Menezes RPB, et al. MolPredictX: Online Biological Activity Predictions by Machine Learning Models. Mol Inform, 2022, 41(12):e2200133. doi: 10.1002/minf.202200133.
35. Gundersen V. Protein aggregation in Parkinson's disease: protein aggregation in Parkinson's Disease." Acta Neurologica Scandinavica, 2010, 122:82-87. doi: 10.1111/j.1600-0404.2010.01382.x.